Generation and Recombination of Defects in Vitreous Silica Induced by Irradiation with a Near-Infrared Femtosecond Laser

Hong-Bo Sun and Saulius Juodkazis

Satellite Venture Business Laboratory, The University of Tokushima, 2-1 Minamijyosanjima, Tokushima 770-8506, Japan

Mitsuru Watanabe, Shigeki Matsuo, and Hiroaki Misawa*

Department of Ecosystem Engineering, Graduate School of Engineering, The University of Tokushima, 2-1 Minamijyosanjima, Tokushima 770-8506, Japan

Junji Nishii

Optical Materials Division, Osaka National Research Institute, 1-8-31 Midorigaoka, Iketa, Osaka 563-8577, Japan

Received: August 11, 1999; In Final Form: December 13, 1999

Properties of defects induced by irradiation with a near-infrared femtosecond laser beam into vitreous silica are reported. Three photoluminescence bands with photon energy of 1.9, 2.7, and 4.4 eV were observed under an excitation of 5.0 eV. An isochronal annealing experiment revealed that unrelaxed oxygen vacancies ODC(II) and interstitial oxygen were generated as dominant species during the irradiation. In the annealing, diffusion of the interstitial oxygen was thermally activated, leading to a direct reduction of oxygen-deficiency-related defects such as ODC(II) and E′ center. The concentration of oxygen-excess-related defects such as peroxy radicals, together with nonbridging oxygen−hole centers, increased first with annealing then decreased with the exhaustion of oxygen and their precursor, the E′ center. The recombination of oxygen vacancies with interstitial oxygen is characterized as the major process occurring during the annealing.

Introduction

Silica-based materials are widely employed in microelectronics[1] and UV optics[2] as well as fiber optics,[3] and point defects play an important role in this regard due to their effects on the chemical and physical properties of the materials.[4] They are not only related to the undesirable degradation of electrical or optical characteristics, but also bring specific features or applications.[4] This has been manifested in the recent development of femtosecond (fs) laser microfabrication techniques,[5−10] in which laser pulses have been used to rapidly and precisely deposit energy in transparent dielectrics.[5,6] With the beam tightly focused, damage spots or lines of micro- and submicrometer sizes are recorded.[5,6] This phenomenon has been used for the preparation of photonic materials and devices such as three-dimensional (3D) optical memory bits,[6,7] total internal reflection optical waveguides,[8] and photonic band gap crystals[9] in silica glass. A storage density in 3D optical memory of as high as 70 GB/cm^3 has been achieved.[6] Furthermore, we have found that the damaged microregion features a strong emission of blue photoluminescence (PL), which can be used for the fluorescence readout of bits.[10] It will be quite interesting if rewritable materials are developed out of silica glass. A general idea we propose is as follows: (i) arrays of bit sites are registered in bulk material by tightly focused laser irradiation and, (ii) single-bit annealing, by which the photoluminescence of specific bits can be effectively annihilated. Representation of the binary "0" and "1" can therefore be accomplished by bits without (annealed bits) and with (unannealed bits) PL emission.

Without a deep understanding of the properties of these defects, these applications will be much hindered. Research on preexisting or irradiation (electron, neutron beam, γ-ray, UV irradiation, etc.) induced defects in crystalline or amorphous silica has been a hot topic for nearly 4 decades.[11−13] For a near-infrared intense femtosecond laser irradiation, defects are introduced by a different mechanism since the energy of photon quanta (1.55 eV for 800 nm wavelength) is much smaller than the band gap width of silica (8.9 eV[14]). A multiphoton absorption[15] is launched due to an extremely high peak power density (∼tens of TW/cm^2). Although the resulting optical damage has been put to use in a number of important applications, the properties of the defects thus induced in silica have not yet been deeply investigated, especially at the level of atoms and molecules.

In this paper, we report the first observation of PL emission of defects induced by near-infrared intense femtosecond laser irradiation, and present the results of our systematic research on the characteristics of point defects using optical absorption (OA), PL, and electron spin resonance (ESR) measurements.

Experimental Section

The configuration of equipment for femtosecond laser irradiation of the silica is similar to that which we have reported previously.[6] Different vitreous silica samples, ED-B, ED-C (brands of dry silica with [OH] < 10 ppm, from Nippon Silica

* Corresponding author. E-mail: misawa@eco.tokushima-u.ac.jp.

10.1021/jp992828h CCC: $19.00
Published on Web 03/23/2000

Glass Co.), and #A ([OH] < 100 ppm, from Sumikin Quartz Products, Inc.), were used. An femtosecond laser system composed of an oscillator (Tsunami, pumped by argon ion laser, from Spectra Physics) and a kilohertz pulse amplifier (Spitfire, also from Spectra Physics) was used as a light source, which produced a laser with a pulse width of 150 fs and a wavelength of 800 nm at a repetition rate of 1 kHz. The laser beam was collimated and directed to an inverted optical microscope (Olympus IX70) and focused into a vitreous silica plate through an oil-immersion objective lens (×100 magnification, and the numerical aperture, NA ~ 1.35). A 0.5 μJ pulse energy was sufficient to introduce visible changes in the transparency 50 μm under the sample's surface. Irradiated voxels (volume elements) with diameters of approximately 1.5 μm were written by single-pulse shots. The sample was translated by a computer-controlled pulsed stage with a maximum scanning speed of approximately 2500 μm/s (LTS-500X, Sigma Koki), which enabled a uniform distribution of bits in the scanning plane (average spot spacing 2 μm in the present samples). The irradiated bits layer was arranged inside the plate, which completely ruled out the possibility of surface ablation effects and contamination in the ensuing process. An atomic force microscope (AFM, SPA-300, Seiko Instruments) was employed to analyze the bit profiles. The samples were annealed in a micro-heater (LK1500, Linkam) equipped with an optical microscope. The maximum available temperature was 1500 °C with an accuracy of ±1 °C, and the rates for increasing and decreasing temperature could be controlled within 1−50 °C/min, and 1−100 °C/min, respectively. The PL and photoluminescence excitation (PLE) spectra were measured by means of a fluorescence spectrometer (FP-4500, Hitachi) equipped with a photomultiplier as a detector and a 150 W Xe lamp as an excitation source. OA was measured with a spectrum photometer (Shimazu UV-3100). Femtosecond spectra were taken with an excitation of the third harmonic of a 750 nm, 120 fs, and 82 MHz laser from a mode-locked Ti:sapphire laser (Tsunami, Spectra Physics) pumped by a solid state laser (Millennia, also from Spectra Physics). After passing through a spectrometer (Acton, ARC300I, 600 grooves/mm, blazing at 500 nm), PL signals were detected by a liquid nitrogen cooled charge-coupled device (LN-CCD, Princeton Instruments, Inc). ESR spectra were measured at 77 K at X-band frequency (Brucker ESP 300E).

Samples from the same fabrication process were annealed, each at a fixed temperature, starting from 100 °C and then rising in steps of 50 °C up to 500 °C, and then at 600 and 1200 °C, for 30 min under a nitrogen atmosphere. To suppress the influences of intermediate processes, the maximum available speeds were used to increase (100 °C/min) and decrease (50 °C/min) the temperature. After cooling to room temperature, the samples were characterized by different techniques including PL, OA, and ESR.

Results and Discussion

1. Generation of Point Defects. The efficiency of multiphoton absorption (MPA) is usually much lower than that of linear absorption. For example, for vitreous silica, we have a linear absorption coefficient of $\alpha_{linear} \sim 1 \times 10^{-3}$ cm^{-1} and a two-photon absorption coefficient of $\beta_{two-photon} < 1.25 \times 10^{-14}$ m/W. In this research, the photochemical reactions responsible for the generation of point defects are very possibly launched by a 6-photon absorption process that is enabled by a very high photon flux density (~10^{32}/cm^2 s by order). The single-shot excitation sequence can be simply described as the follows: (i) electrons are initially excited to antibonding bands, then become free carriers by MPA; (ii) they further acquire kinetic energy through a sequential linear absorption from the same pulse; (iii) these excited electrons transfer the excess energy to valence electrons by impact ionization, exciting new electron−hole pairs; and (iv) the newly generated electrons undergo a similar linear absorption of photons, and this process continues as an avalanche. The electrons are excited faster than they can transfer their excess energy to the lattice. Therefore, the highly excited and tightly localized plasma expands in an explosive way, generating a hole surrounded with a more densified phase. Microcosmically, Si−O covalent bonds were violently broken and defects were generated through series of photochemical reactions (see Figure 5, below). *The defects discussed in this paper should exist abundantly in the surrounding region*. Figure 1a shows an optical microscopic (OM) image of a voxel layer (left) and an AFM image (right) of a single voxel introduced by a single-pulse shot. From AFM measurement, the occurrence of a void region (and therefore the surrounding densification) was confirmed, and its volume was excluded from the bulk for the estimation of defect concentrations.

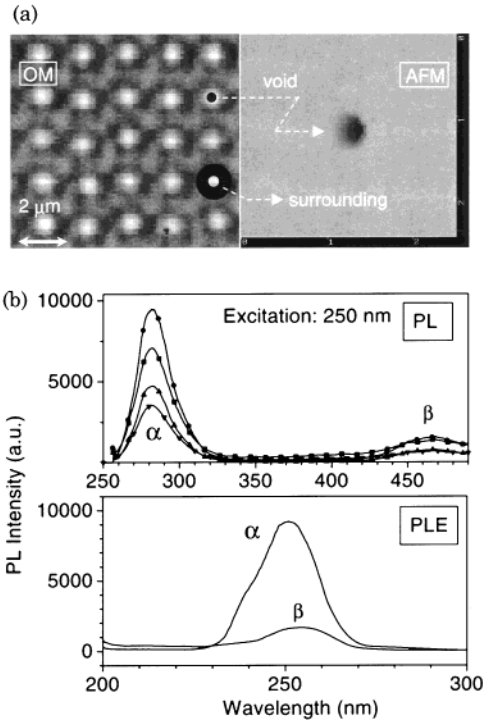

Figure 1. Intense femtosecond laser irradiation-induced damages in vitreous silica by single pulse shots. The pulse width is 150 fs (FWHM), and the repetition rate is 1 kHz. Under focusing by objective lens with 100 times of magnification and 1.35 of NA, the pulse energy 0.5 μJ corresponds to a laser power density of ~10^{18} W/cm^2. (a) Optical microscopic (OM) and AFM images of damaged voxels. For AFM scanning, the sample was polished. (b) PL and PLE spectra measured before annealing with an excitation of a 150 W xenon lamp. The two PL bands are termed as α and β for a convenience of peak recognition in all figures. The symbols in the PL spectra of (b) denote different samples and irradiation laser wavelength: (●) #A, 800 nm; (■) ED-B, 800 nm; (▲), #A, 400 nm; (▼) ED-C, 800 nm.

2. Photoluminescence Features of As-Irradiated Samples. As an attempt at clarifying the origins of possible species, photoluminescence, optical absorption, and ESR measurements were made before irradiation. No intrinsic defect features were detectable with preirradiated samples by the enumerated techniques, implying that the defects, if they emerged after laser exposure and the following annealing, were extrinsic. To sketch all the possible fluorescence characteristics of the damaged

silica, PL-PLE mapping was carried out at room temperature, 22 °C. Two PL bands peaking at 282 nm (4.4 eV band, full width at half-maximum, FWHM ~ 0.35 eV) and 468 nm (2.7 eV band, FWHM ~ 0.32 eV) were observed with exactly the same excitation wavelength, 250 nm (5.0 eV), as shown in Figure 1b. Accurate form factors of peak positions and FWHMs allow an assignment of the defects. Optical excitation bands at 5.0 eV[11,12] (B_2, or $B_{2\alpha}$) and 7.6 eV[11,12] (E band) with PL bands at 2.7 and 4.4 eV have been associated with oxygen deficiency in high-purity silica. In addition, it is now well accepted that B_2 and E bands involve transitions from two distinct configurations of the same center, the relaxed and unrelaxed oxygen vacancies ODC(I) and ODC(II), respectively.[16] ODC(I) was not investigated in this study due to the lack of vacuum ultraviolet techniques. However, the 5.0 eV band accompanied by 2.7 and 4.4 eV PL was already a sufficient signature of ODC(II). From the descriptions above, we can come to a preliminary conclusion that the defects induced by infrared femtosecond laser exposure behave similarly to those induced by other kinds of irradiation.[11,12]

Strong $B_{2\alpha}$ absorption indicates the existence of a high concentration of ODC(II), which was introduced here only by IR laser irradiation through a multiphoton absorption process. A void surrounded with densified crust region occurred in the focal point, implying an intense local structural variation. Si−O bonds can be broken due to the excitation of σ electrons, accompanied by the generation of an Si−Si bond and interstitial oxygen. The oxygen atoms ejected from normal Si−O−Si bond sites combined into molecules, $2O_i \rightarrow (O_2)_i$. The O_2 molecules, distributed in the neighborhood of the ODC(II) were inevitably frozen in the silica matrix by a subsequent temperature quenching because the exposure duration was extremely short, e.g., a subpicosecond time domain. The high chemical potential from oversaturated oxygen concentration will offer a driving force for a restoration of material (to a denser phase; for details see discussions in the last paragraph), at a rate that would be expected to accelerate with increased temperature.

3. Photoluminescence and Optical Absorption versus Annealing. Much more information on the recognition and interchange of the defects was obtained from the annealing analysis. Figure 2 shows the annealing properties of the fluorescence intensity of different PL bands. Apart from approximately exponential decays of PL intensity with the annealing, no new species were observed up to 1200 °C. Shown in Figure 2a is the evolution of the PL spectra with temperature, and the corresponding peak intensity variations versus the inverse of temperature are presented in Figure 2b. After 30 min of annealing, the PL intensity was almost unchanged at $T <$ 200 °C. A significant attenuation of PL started from 300 °C, and it was almost absent at 500 °C. The underlying concept of this variation is that the concentration of ODC(II), which is responsible for the two PL emissions, is reduced by the annealing.

Because ODC is a diamagnetic defect and thus invisible to ESR techniques, the OA spectra give the most direct evidence regarding the change in the concentration of ODC(II) with heating. Shown in Figure 3 are the absorption spectra from the samples annealed under various temperatures, and the corresponding temperature-dependent OA intensity is illustrated in Figure 2b. Decays of OA are quite similar to those of both PL bands, showing that ODC(II) is the dominant defect species. This conclusion is further supported by the fact that no other OA bands are discernible except for a weak absorption at 5.8 eV, which can only be attributed to an E′ center (or SiE′, ≡Si•,

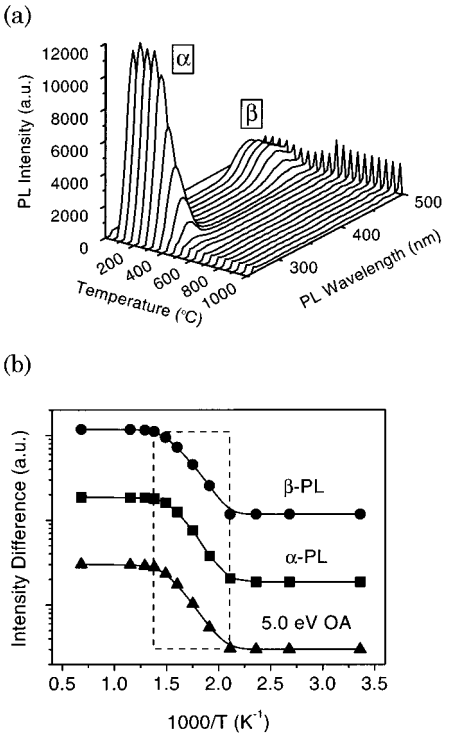

Figure 2. Annealing *T*-dependent PL and OA characteristics. The rates for temperature increase and decrease were 50 and 100 °C/min, respectively. The samples were protected in a N_2 flow during annealing, kept in a certain temperature for 30 min at each stage. (a) An evolution of PL spectra, and (b) intensity of PL and OA versus $1/T$ (T is temperature in kelvin). The OA intensity is abstracted from Figure 3.

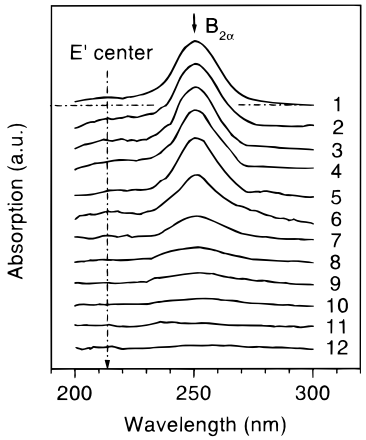

Figure 3. OA spectra at different temperatures (1, 25; 2, 100; 3, 150; 4, 200; 5, 250; 6, 300; 7, 350; 8, 400; 9, 450, 10, 500; 11, 600; and 12, 1200 °C). 5.0 eV band is undoubtedly assigned to ODC(II), while the weak absorption at 5.8 eV is from E′ center.

oxygen vacancy-related defects with an unpaired spin that is denoted here by a dot "•") from its form factors[11,12] (peak position ~5.8 eV and FWHM ~0.8 eV). The bands at both 5.0 and 5.8 eV almost disappeared after annealing at 500 °C. On the basis of the history of its creation, its highest concentration, and the consistent tendency of its PL and OA against annealing (Figure 2b), the significant (ODC(II)) decrease with the increase of annealing temperature can be best interpreted as due to its recombination with interstitial oxygen.

The concentration of ODC(II) is roughly estimated according to the formula[17] $Nf = \beta\alpha_0^{\max}\Delta E$, where N (cm^{-3}) is the defect concentration, provided that the density is small enough to ignore the interaction between the defects, α (cm^{-1}) is the absorption coefficient at maximum wavelength ($\alpha_0^{250\ nm} \sim 16.8$

cm^{-1} for ODC(II) and $\alpha_0^{213\ nm} \sim 1.5\ cm^{-1}$ for SiE′; both depend on the laser pulse energy and density of voxels, and therefore, concentration of defects), $\beta \sim 1.3 \times 10^{18}\ eV^{-1}\ cm^{-2}$ is an empiric constant, and ΔE (eV) is the absorption line width ($\Delta E_{ODC(II)} \sim 0.42$ eV, and $\Delta E_{SiE'} \sim 0.8$ eV). Oscillator strength is denoted by f (dimensionless constant, ~1, for deep centers). With the parameters determined from the experiment, the concentration of ODC(II) was calculated to be [ODC(II)] ~ $9.3 \times 10^{17}\ cm^{-3}$. Actually, the absolute concentration obtained here was quite rough. What we can expect with higher accuracy is the concentration ratio of two defects, for which we get [ODC(II)]/[SiE′] ~ 6.

4. Electronic Spin Resonance Measurement. The SiE′ center was originally reported by Weeks,[18] and this center has been observed to exist in several variants,[19] which are the best-known color centers in irradiated silica glasses. ODC(II) is commonly considered to be a precursor of SiE′.[11,12] Since we have observed an intense absorption band due to ODC(II) and a weak absorption band due to E′, it is natural to ask whether a more effective and direct means can be offered to investigate the latter. It is also necessary to determine other possible defects, since it has been observed that nonbridging oxygen−hole center (≡Si−O•, NBOHC) and peroxy radical (≡Si−O−O•, POR) are generated in γ-ray irradiated samples accompanying the cleavage of Si−O bonds.[20] ESR measurements have allowed for the direct observation of dangling bond type defects such as POR, NBOHC, and E′ centers. Figure 4 shows the ESR spectra of samples before and after annealing at certain temperatures. The E′ center signal can be clearly observed in fresh irradiated samples under microwave power of 0.02 mW and a field modulation of 0.63 G (Figure 4a). The spectra quite resemble those reported[20] for oxygen-deficiency-related (ODR) SiO_2 irradiated by 6.4 and 7.9 eV laser photons, characterized by the spectroscopic splitting factor, with g values of $g_1 = 2.0018$, $g_2 = 2.0006$, and $g_3 = 2.0003$. After annealing at 400−500 °C, the SiE′ signal is scarcely detectable, and the remaining ESR response can be ascribed to POR on the basis of a comparison of the principal g values[22] to those of well-accepted data: $g_1 = 2.0014$, $g_2 = 2.0074$, and $g_3 = 2.067$, as shown in Figure 4b, recorded with 5 mW of microwave power and a field modulation of 5.0 G. NBOHC,[22] with its $g = 2.0095$, was not detectable or was obscured by a much stronger POR signal. However, the formation of NBOHC was suggested by the generation of a PL band at 1.9 eV after femtosecond laser irradiation, which will be shown in Figure 6.

Figure 4c illustrates an annealing T dependence for the ESR signals of the different defects, all of which have been calibrated to be proportional, by the same factor, to the absolute defect concentration. The decrease in the SiE′ concentration versus an increase in the annealing temperature is consistent with the intensity change of the 5.8 eV band in the OA measurement. The POR concentration, on the other hand, first increases with temperature, and then reaches a maximum at approximately 450 °C (deduced from the spline-fitted curve), and then decreases rapidly. These phenomena can be understood as follows [see Figure 5]:

1. During the femtosecond laser irradiation, ODC(II), SiE′ and interstitial oxygen (atom or molecule) are formed, and some of the interstitial oxygen reacts with SiE′ followed by the formation of PORs.

2. The concentration of PORs maximizes in response to the thermal annealing at 450 °C, while ODC(II) and SiE′ almost disappear, which means that the excess oxygen reacts with ODC(II), resulting in a nondefective SiO_2 matrix.

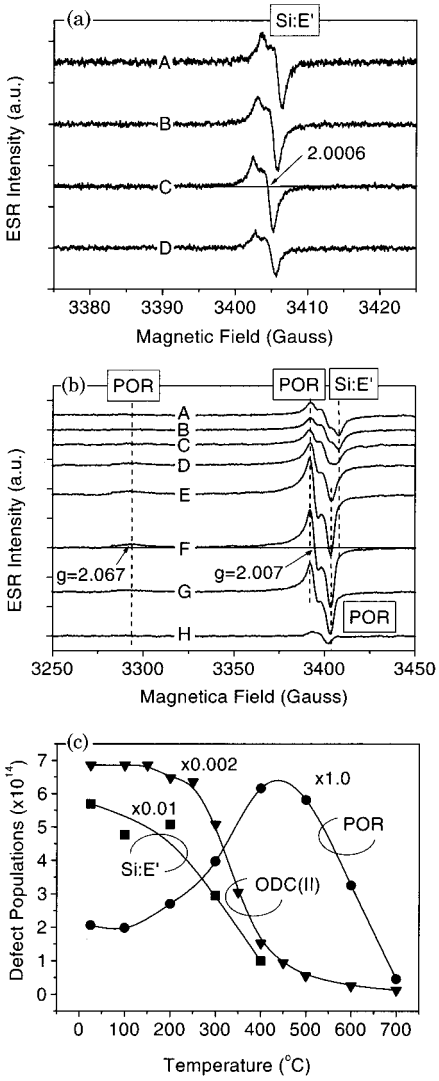

Figure 4. ESR spectra of samples annealed at different temperatures, which were recorded at X band and 77 K. Letters denote conditions of as-fabricated (A), and (B) 100, (C) 200, (D) 300, (E) 400, (F) 500, (G) 600, and (H) 700 °C annealing. Spectra measured at (a) the microwave power of 0.02 mW, and the field modulation of 0.63 G and (b) at the microwave power of 5 mW and the field modulation of 5.0 G; (c) defect populations versus temperature, where, for the POR and E′, spin numbers are shown, while ODC(II) population was calculated from its ratio with E′ as indicated by previous paragraph.

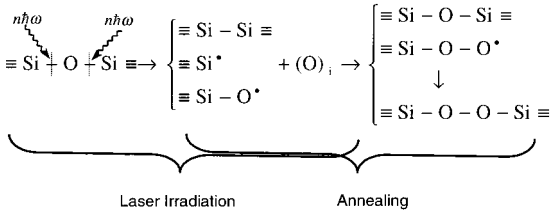

Figure 5. Schematic photochemical reactions during femtosecond laser irradiation and annealing. The meaning of symbols is described in the relevant text.

3. In the second stage, almost all defects are diminished after annealing above 700 °C, while the laser-damaged area clearly remains, based on observations with an optical microscope.

Pfeffer[23] and Tsai[24] et al. have observed a one-to-one conversion from SiE′ to POR; in our case, however, the efficiency is on the order of 1%, as calculated by $([POR]_{max} - [POR]_{initial})/([SiE']_{initial} - [SiE']_{end})$. As the annealing proceeded, E′ was continuously consumed, with part of it being converted

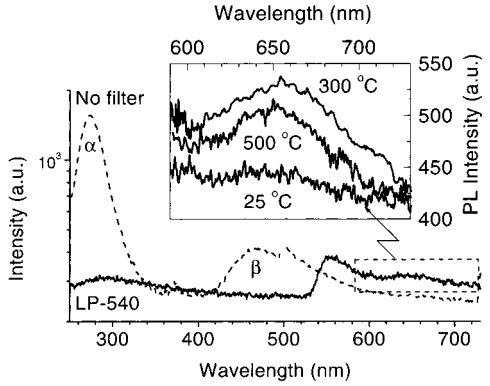

Figure 6. PL spectra under a femtosecond laser excitation. Filter of long-pass 540 nm (LP540) were used to screen out the second and third spectral order of the 2.7 and 4.4 eV PL bands. As a comparison, the spectrum taken without any filter is also shown. The inset is zoomed in from the spectral region of NBOHC PL band.

to oxygen-excess-related (OER) defects, including POR. [SiE′] was ultimately lowered to a level at which further conversion became negligible. One of the origins of the decrease in [POR] above 450 °C might be its conversion to peroxy linkage (≡Si−O−O−Si≡, POL), which is a stable defect in silica.[20]

5. Further Evidence from NBOHC. It has now been established from the previous discussion that POR was generated in the laser irradiation and that its concentration increase was due to the recombination of oxygen with E′. The presence of another important species, NBOHC, generally arising from the breakage of Si−O bonds, was not confirmed by ESR measurement. However, the femtosecond laser-excitation PL spectra not only demonstrate the existence of NBOHC but also show NBOHC to behave similarly to POR in annealing. Figure 6 shows the PL curves under femtosecond laser excitation, in which long-pass filters (370 and 540 nm) were used to erase the disturbance from high-order spectra. As expected, the 2.7 and 4.4 eV bands showed the same annealing tendency as that observed in Xe lamp excitation spectra (Figures 1 and 2). A new PL band emerges at 650 nm (1.9 eV band), which can be attributed to NBOHC[11,12] based on its characteristics of 4.8 eV excitation, as well as PL peak position and a FWHM of approximately 0.8 eV. The NBOHC concentration increases first with annealing temperature, then saturates and decreases, showing the same tendency as the ESR signal of POR.

Additional evidence to support the above analysis (subsections I−V) can be offered by directly measuring the concentration of interstitial oxygen. Skuja et al.[25] have detected the presence of interstitial oxygen molecules in SiO_2 glass by direct 1064.1 nm photon excitation ($(\upsilon'' = 0) \rightarrow (\upsilon' = 1)$) of the forbidden O_2 molecule $^1\Delta_g(\upsilon'=0) \rightarrow {}^3\Sigma_g(\upsilon''=0)$ luminescence at 1227 nm. The detection of interstitial oxygen is an obvious target for future research.

As indicated by Figure 4c and Figure 6, 700 °C annealing has diminished all the defects addressed in this research, while the voxels are kept unchanged under optical microscope (see Figure 1a) but leaving a permanent refractive index change. It can be understood from well-documented experimental and theoretical (computer simulation) studies[26] showing silica structures consisting of tetrahedral [SiO_4] coordination can undergo a variety of temperature- and pressure-induced transformations, especially those of the amorphous form. A 1.4% volume shrinkage has been observed[27] in electron-irradiated (2×10^{12} rad) vitreous silica and Hugobiot shock experiment[28] gave more than 50% densification (<30 GPa). These demonstrated the existence of denser phases of silica networks. In the case of femtosecond laser explosion in silica, a rough estimation based on electron plasma model gives a local temperature rise of 10^6 K and pressure larger than 100 GPa, which can easily lead to such denser phases (but with a high concentration of defects) through a reconstructive transformation. The material quality is improved by the annealing through the recombination of defects, possibly accompanied by a displacive transformation since both do not require as much energy. Actually, annealing is almost a routine procedure for growing semiconductor materials to minimize the nonperfection of crystals.

It is noteworthy that all the figures in this paper are from #A samples irradiated by laser at a wavelength of 800 nm (in Figure 1, we give PL spectra from different samples and irradiation laser wavelengths). However, the same phenomena have been almost quantitatively observed in all three kinds of silica damaged by both 400- and 800 nm irradiation, indicating that our conclusion regarding the generation and variation mechanisms of defects induced in silica by focused femtosecond laser can be generalized.

Summary and Conclusion

In addition to its technological importance, femtosecond laser irradiation is distinguished from other forms of irradiation (e.g., electron, neutron, γ-ray, deep UV) for its unique features as follows. (i) Much smaller irradiation quanta (sub-bandgap), but leading to more intense structural modifications of materials, i.e., occurrence of void and more-densified phase. (ii) Irradiation regions were confined inside materials due to the MPA process. During irradiation and annealing, the materials are stoichiometrically unchanged and foreign contamination is impossible to be introduced. Such a condition is highly desired, but not available elsewhere, for the characterization of defects.

We report in this paper, to the best of our knowledge, a first observation of PL and PLE characteristics of defects induced by optically or near-infrared femtosecond lasers in silica glass. In the meantime, we present a detailed dynamics on the generation and recombination of the photogenerated defects as speculated as follows.

1. Three PL bands peaking at 1.9, 2.7, and 4.4 eV under 5.0 eV excitation were simultaneously observed in intrinsic silica due to visible (400 nm) and near-infrared (800 nm) intense femtosecond laser irradiation. With well-defined spectra form factors (peak positions and FWHMs), the 5.0 eV OA with germinated 2.7 and 4.4 eV can be assigned with confidence to an unrelaxed oxygen vacancy, ODC(II), and the 1.9 eV band can be assigned to NBOHC.

2. The presence of an interstitial oxygen molecule is inferred from the generation of ODC(II) from defect-free stoichiometry vitreous silica and solidified by the concentration increase of POR and NBOHC species in 30 min annealing (T < 450 °C). Therefore, the intense femtosecond laser irradiation-induced damage mechanism features a strong radiolytic process, wherein oxygen atoms are displaced in the course of the decay of electronic excitation. The interstitial oxygen plays an important role in the transformation of defects.

3. There are different pathways for the recombination of oxygen molecules with E′. The conversion efficiency from E′ to POR is approximately 1%, much lower than that from other irradiation. These results suggest that the ODC(II) is the dominant defect species after irradiation and that the recombination of interstitial oxygen with ODC(II) is the major process in annealing. It seems that a direct restoration to normal Si−O bonds is much favored, while only a small percentage of SiE′ is converted to OER defects.

Acknowledgment. This work has been supported in part by a Grant-in-Aid for Scientific Research (A)(2) from the Ministry of Education, Science, Sports, and Culture (09355008), the Marubun Research Promotion Foundation, and the Satellite Venture Business Laboratory of the University of Tokushima.

References and Notes

(1) See, for example: Warren, W. L.; Poindexter, E. H.; Offenberg, M.; Muller-Warmuth, M. *J. Electrochem. Soc.* **1992**, *139*, 872.

(2) (a) Poumellec, B.; Kherbouche, F. *J. Phys. III* **1996**, *6*, 1595. (b) *Complex behaviour of glassy systems*; Rubi, M., Perez-Vicente, C., Eds.; Springer: Berlin/New York, 1997.

(3) Atkins, R. M.; Mizrahi, V.; Erdogan, T. *Electron. Lett.* **1993**, *29*, 385.

(4) Griscom, D. L.; Brown, D. B.; Saks, N. S. In *The Physics and Chemistry of SiO_2 and Si−SiO_2 Interface*; Helms, C. R., Deal, B. E., Eds.; Plenum Press: New York, 1988; p 287.

(5) Glezer, E. N.; Mazur, E. *Appl. Phys. Lett.* **1997**, *71*, 882.

(6) Watanabe, M.; Sun, H.−B.; Juodkazis, S.; Takahashi, T.; Matsuo, S.; Suzuki, Y.; Nishii, J.; Misawa, H. *Jpn. J. Appl. Phys.* **1998**, *37*, L1527.

(7) Glezer, E. N.; Milosavljevic, M.; Huang, L.; Finlay, R. J.; Her, T.-H.; Callan, J. P.; Mazur, E. *Opt. Lett.* **1996**, *21*, 2023.

(8) Miura, K.; Qiu, J.; Inouye, H.; Mitsuyu, T.; Hirao, K. *Appl. Phys. Lett.* **1997**, *71*, 3329.

(9) Sun, H.-B.; Xu, Y.; Matsuo, S.; Misawa, H. *Opt. Rev.* **1999**, *6*, 396.

(10) Watanabe, M.; Juodkazis, S.; Sun, H.-B.; Matsuo, S.; Misawa, H. *Appl. Phys. Lett.* **1999**, *74*, 3957.

(11) Griscom, D. L.; Ceram, J. *Soc. Jpn.* **1991**, *99*, 923, and literature therein.

(12) Skuja, L. *J. Non-Cryst. Solids* **1998**, *239*, 16 and literature therein.

(13) Zhang, G.; Mao, Y.; Thomas, K. *J. Phys. Chem. B* **1997**, *101*, 7100.

(14) Phillipp, H. R. *Solid State Commun.* **1966**, *4*, 73.

(15) Stuart, B. C.; Feit, M. D.; Rubenchik, A. M.; Shore, B. W.; Perry, M. D. *Phys. Rev. Lett.* **1995**, *74*, 2248.

(16) (a) Nishikawa, H. *Phys. Rev. Lett.* **1985**, *72*, 2102. (b) Tohmon, R.; Shimogaichi, Y.; Mizuno, H.; Ohki, Y. *Phys. Rev. Lett.* **1989**, *62*, 1388.

(17) Böer, K. W. *Survey of Semiconductor Physics, Vol. I*; Reprinted by World Publishing Corp.: Beijing, 1994; p 506.

(18) Weeks, R. A.; J. *Appl. Phys.* **1956**, *27*, 1376.

(19) Griscom, D. L. *Nucl. Instrum. Methods Phys. Res.* **1984**, *Sect. B1*, 481.

(20) (a)Devine, R. A.; Arndt, *J. Phys. Rev. B* **1987**, *35*, 770. (b) Devine, R. A.; Arndt, *J. Phys. Rev. B* **1989**, *39*, 5132.

(21) Nishikawa, H.; Nakamura, R.; Ohki, Y. *Phys. Rev. B* **1993**, *48*, 15584.

(22) Stapelbroek, M.; Griscom, D. L.; Friebele, E. J.; Sigel, G. H.; Jr, *J. Non-Cryst. Solids* **1979**, *32*, 313.

(23) Pfeffer, R. L. In *The Physics and Chemistry of SiO_2 and the Si−SiO_2 Interface*; Helms, C. R., Deal, B. E., Eds.; Plenum: New York, 1988; p 169.

(24) Tsai, E.; Griscom, D. L. *Phys. Rev. Lett.* **1991**, *67*, 2571.

(25) Skuja, L.; Güttler, B. *Phys. Rev. Lett.* **1996**, *77*, 2093.

(26) Murashov, V. V.; Svishchev, I. M. *Phys. Rev. B* **1998**, *57*, 5639.

(27) Dellin, T. A.; Tichenor, D. A.; Barsis, E. H. *J. Appl. Phys.* **1977**, *48*, 1131.

(28) *LANL Shock Hugoniot Data*; Marsh, S. P., Ed.; University of California Press: Berkeley, CA, 1980.